SLAC-PUB-5861
November 1992
(T/E)

Measurements of the Electric and Magnetic Form Factors of the Neutron from $Q^2 = 1.75$ to 4.00 $(\mathrm{GeV/c})^{2\star}$

A. Lung,[1,a] L. M. Stuart,[2,4,b] P. E. Bosted,[1] L. Andivahis,[1]
J. Alster,[12] R. G. Arnold,[1] C. C. Chang,[5] F. S. Dietrich,[4] W. R. Dodge,[7,c]
R. Gearhart,[10] J. Gomez,[3] K. A. Griffioen,[8] R. S. Hicks,[6] C. E. Hyde-Wright,[13]
C. Keppel,[1] S. E. Kuhn,[11,d] J. Lichtenstadt,[12] R. A. Miskimen,[6] G. A. Peterson,[6]
G. G. Petratos,[9,b] S. E. Rock,[1] S. H. Rokni,[6,b] W. K. Sakumoto,[9]
M. Spengos,[1] K. Swartz,[13] Z. Szalata,[1] L. H. Tao[1]

[1] *The American University, Washington D.C. 20016*
[2] *University of California, Davis, California 95616*
[3] *CEBAF, Newport News, Virginia 23606*
[4] *Lawrence Livermore National Laboratory, Livermore, California 94550*
[5] *University of Maryland, College Park, Maryland 20742*
[6] *University of Massachusetts, Amherst, Massachusetts 01003*
[7] *National Institute of Standards and Technology, Gaithersburg, Maryland 20899*
[8] *University of Pennsylvania, Philadelphia, Pennsylvania 19104*
[9] *University of Rochester, Rochester, New York 14627*
[10] *Stanford Linear Accelerator Center, Stanford, California 94309*
[11] *Stanford University, Stanford, California 94305*
[12] *University of Tel-Aviv, Ramat Aviv, Tel-Aviv 69978, Israel*
[13] *University of Washington, Seattle, Washington 98195*

Submitted to Physical Review Letters

⋆Work supported in part by National Science Foundation grants PHY–87–15050 (AU), PHY–89–18491 (Maryland), PHY–88–19259 (U Penn), and PHY–86–58127 (UW); by Department of Energy contracts DE–AC03–76SF00515 (SLAC), W–7405–ENG–48 (LLNL), DE–FG02–88ER40415 (U Mass), DE–AC02-ER13065 (UR) and DE–FG06–90ER40537 (UW); and by the US–Israel Binational Science Foundation.

ABSTRACT

Quasielastic e–d cross sections have been measured at forward and backward angles. Rosenbluth separations were done to obtain R_L and R_T at $Q^2 = 1.75$, 2.50, 3.25 and 4.00 $(\mathrm{GeV/c})^2$. The neutron form factors, G_{En} and G_{Mn}, have been extracted using a non-relativistic model. The sensitivity to deuteron wave function, relativistic corrections, and models of the inelastic background are reported. The results for G_{Mn} are consistent with form factor scaling, while G_{En} is consistent with zero. Comparisons are made to theoretical models based on VMD, PQCD and QCD sum rules, as well as constituent quarks.

New measurements of the neutron electromagnetic form factors, $G_{En}(Q^2)$ and $G_{Mn}(Q^2)$, are reported. These form factors are of fundamental importance in understanding nucleon structure, as well as for calculations of processes involving the electromagnetic interaction with complex nuclei. Using fits to early form factor data, Vector Meson Dominance (VMD) models[1] make predictions for the form factors in the low four-momentum transfer squared, Q^2, region. Models based on dimensional scaling and Perturbative Quantum Chromodynamics (PQCD) are used to describe[2] the form factors at high Q^2. To describe the behavior at intermediate values of Q^2, a hybrid model[3] by Gari and Krümpelmann (GK) uses VMD fits to low Q^2 data, which are constrained to agree with PQCD results at high Q^2. Other models which predict form factor behavior are QCD sum rules,[4] and constituent quark models.[5]

Previous measurements[6] of the elastic electron–neutron cross sections have been made at forward angles up to $Q^2 = 10$ (GeV/c)^2. Combining these measurements with backward angle data[7] has allowed Rosenbluth separations of G_{En} and G_{Mn}, but only up to $Q^2 = 2.7$ (GeV/c)^2. Several factors have permitted improvements in the range and precision of measurements of the nucleon form factors. The Nuclear Physics Injector at SLAC provided a higher intensity, higher energy beam than was available to previous experiments. This sufficiently increased count rates at higher Q^2 to allow cross sections to be measured with 1% statistical errors. Improvements in systematic errors were obtained by measuring the proton form factors through elastic e–p scattering in the same experiment.[8] The most significant improvement over previous experiments was the use of two magnetic spectrometers, one on each side of the beam line, which detected scattered electrons simultaneously. A large solid angle, 1.6 GeV/c spectrometer was fixed at 90° to measure the low-rate, backward-angle cross sections with central momentum, E', between 0.5 and 0.8 GeV/c. The SLAC 8 GeV/c spectrometer detected electrons at central scattering angles, θ, between 15° and 90°, and momentum between 0.5 and 7.5 GeV/c.

The experiment consisted of quasielastic e–d cross section measurements at beam energies, E, from 1.5 to 5.5 GeV and average currents from 0.5 to 10 μA. The beam angle and position were determined to within 0.05 mr and 1 mm, respectively. The total incident charge was measured to an accuracy of 0.5% by two toroidal charge monitors which were calibrated before every data run. The cryogenic liquid deuterium target consisted of a 15 cm long aluminum cylinder, 7 cm in diameter, with 0.1 mm thick walls and endcaps. A similar cell of liquid hydrogen was used to measure the e–p cross sections, and an aluminum target of equivalent radiation length was used to measure endcap contributions. The average density was determined with point-to-point fluctuations of 0.2% and an overall normalization of better than 1%.

Similar detector arrays were used in both spectrometers. Threshold gas Čerenkov counters and lead glass shower counters were used to identify electrons in the presence of pions and other backgrounds. Wire chambers and plastic scintillators were used to measure particle trajectories. The shape of the acceptance for both spectrometers was determined through Monte Carlo simulations and checked against measured e–p cross sections. Details on the detectors and acceptance functions have been previously reported.[8]

Quasielastic e–d spectra at each kinematic point were obtained as a function of missing mass squared, $W^2 = M^2 + 2M(E - E') - Q^2$, where M is the nucleon mass, at fixed θ by dividing the measured counts by the spectrometer acceptance. Subtractions were made for a background contamination of pions (typically 0.2%), and for electrons originating from pair-production in the target. The latter was measured in separate runs by reversing the polarity of the spectrometers, and was 3.5% in the worst case at $Q^2 = 4.0$ (GeV/c)^2 and $\theta = 90^\circ$. Target endcap contributions, present only in the 8 GeV/c spectrometer, were typically 2%.

Spectra were measured at forward and backward angles for $Q^2 = 1.75$, 2.50, 3.25, and 4.00 $(\mathrm{GeV/c})^2$. The typical ϵ range was from 0.2 to 0.9, where $\epsilon = [1 + 2(1+\tau')\tan^2(\theta/2)]^{-1}$ is the longitudinal polarization of the virtual photon, with $\tau' = \nu^2/Q^2$, and $\nu = E - E'$. Data was measured at four ϵ values for each of the two lowest Q^2 points, and at three and two ϵ values for $Q^2 = 3.25$ and 4.00 $(\mathrm{GeV/c})^2$, respectively. The quasielastic peak was clearly visible at $W^2 = M^2 = 0.88$ $(\mathrm{GeV})^2$ for each spectrum, with inelastic contributions at the peak increasing with Q^2 to a maximum of 15% at $Q^2 = 4.00$ $(\mathrm{GeV/c})^2$.

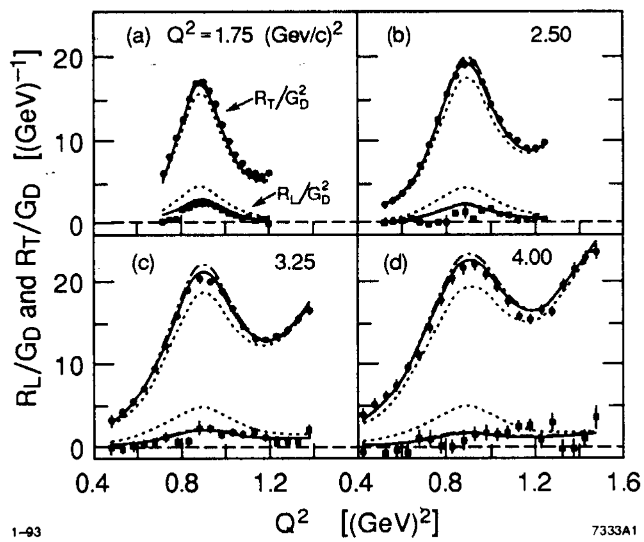

Figure 1. Separated R_T/G_D^2 (circles) and R_L/G_D^2 (squares) for e–d scattering at the four Q^2 values of this experiment. The Q^2 values are at the quasielastic peak and vary slightly with W^2. The errors are statistical only. See text for description of curves.

The measured e–d cross sections per nucleon, $\sigma(E, E', \theta)$, were converted to reduced cross sections, defined as:

$$\sigma_R = \epsilon(1+\tau')\frac{\sigma(E,E',\theta)}{\sigma_{Mott}} = R_T + \epsilon R_L$$

where $\sigma_{Mott} = \alpha^2 \cos^2(\theta/2)/4E^2 \sin^4(\theta/2)$. Rosenbluth separations were done using linear fits to the reduced cross sections for each W^2 value at each Q^2. A normalized longitudinal response function, R_L/G_D^2, was obtained from the slope, and a transverse response function, R_T/G_D^2, from the intercept, where $G_D = (1 + Q^2/0.71)^{-2}$ is the dipole fit. Figure 1 shows the separated data with statistical errors for each of the four Q^2 values of this experiment. The solid curves are model calculations of the combined quasielastic and inelastic contributions. The quasielastic component was modelled with a non-relativistic Plane Wave Impulse Approximation (PWIA) calculation[9] using the Paris deuteron wave function.[10] The proton form factors measured in this experiment were used, with $G_{En} = 0$ and $G_{Mn} = (\mu_n/\mu_p)G_{Mp}$, where $\mu_n = -1.913$ and $\mu_p = 2.793$. The inelastic portion was calculated using a fit to the measured proton resonance region data which was convoluted with the deuteron wave function using a Fermi-smearing model[11] with an impulse approximation based on light-cone dynamics (Inel1). The smeared cross sections were fit to the deuterium data in the resonance region assuming two parameters: the ratio of neutron and proton cross sections, σ_n/σ_p, for resonance production, and for nonresonant background production. The dash-dot curves in Fig. 1 represent a similar calculation, except a relativistic PWIA model by Gross[12] was used. The dotted curves were calculated with the same models as the solid curves, except that the GK parametrization of G_{Mn} and G_{En} were used. The relativistic effects are small compared to the sensitivity to the neutron form factor parametrization, and the data is best described by $G_{Mn} = (\mu_n/\mu_p)G_{Mp}$ and $G_{En} = 0$.

To extract the neutron form factors, R_L and R_T were fit with the model shapes for both the quasielastic and inelastic contributions. In the PWIA, the quasielastic portion of R_L is proportional to $(G_{Ep}^2 + G_{En}^2)$, and R_T is proportional to $(G_{Mp}^2 + G_{Mn}^2)$. The neutron form factors were determined by subtracting the proton form

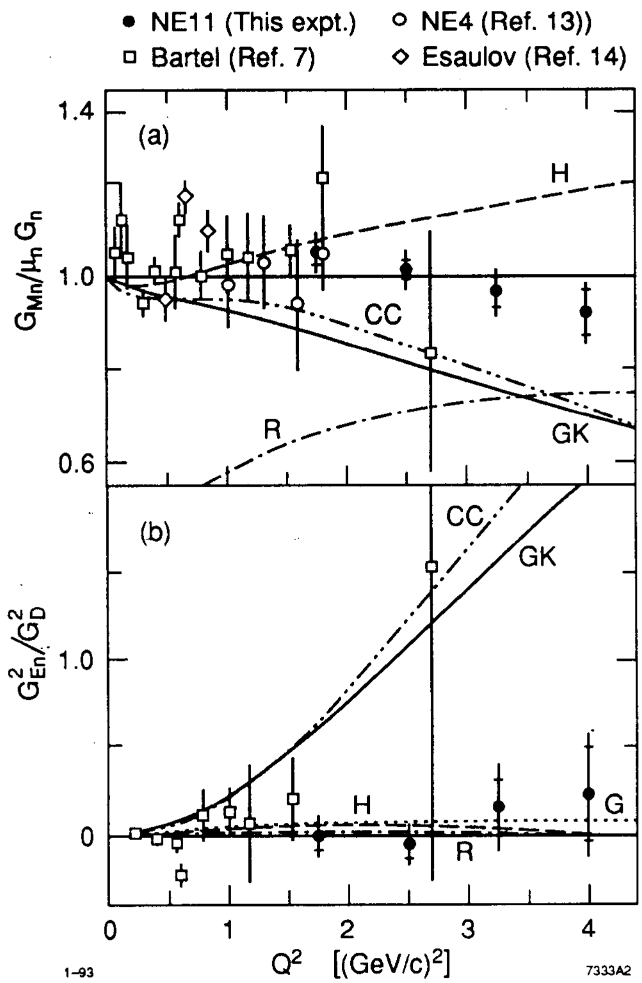

Figure 2. Results for a) $G_{Mn}/\mu_n G_D$ and b) G_{En}^2/G_D^2 versus Q^2 extracted using a non-relativistic quasielastic model, the Paris wave function, and inelastic model (Inel1). The inner error bars are statistical, and the outer include point-to-point and absolute systematic errors. Also shown are previous data [7,13,14], and curves from various fits and predictions which are described in the text.

factors measured in this experiment[8] from the coefficients of the quasielastic fits. The neutron form factors extracted using a non-relativistic PWIA model with the Paris wave function, and inelastic model (Inel1) are shown in Fig. 2 and listed in

Table I. The inner error bars are statistical only, while the outer error bars include systematic errors. The point-to-point errors include the combined uncertainties in beam energy (0.05%) and scattering angle, 0.005° and 0.050° for the 8 GeV/c and 1.6 GeV/c spectrometers, respectively. The absolute systematic errors result from uncertainties in absolute values of the incident charge, radiative corrections, and solid angles of the spectrometers, as well as the absolute normalization of the proton form factors.

Figures 2a and 2b show $G_{Mn}/\mu_n G_D$ and G_{En}^2/G_D^2 respectively, along with previous data[7,13,14] and various theoretical predictions. The new data is in good agreement with previous data where there is overlap. The VMD model shown (H, dashed) from Höhler,[1] is in reasonable agreement with the G_{En} data, but overestimates G_{Mn}. The GK model (solid), which predicts $F_{1n} = 0$, or $G_{En} = \tau G_{Mn}$ where $\tau = Q^2/4M^2$, is in very poor agreement with the new data for G_{En}, and underestimates G_{Mn}. A relativistic constituent quark model (CC, dash-dot-dot) from Chung and Coester[5] also predicts $F_{1n} \approx 0$ and is similarly ruled out. The QCD sum rule predictions (R, dash-dot) from Radyushkin[4] are in reasonable agreement with the G_{En} data, and agreement with G_{Mn} is approached at the highest Q^2 where the calculation is expected to become valid. An additional curve (G, dots) from Galster[15] for G_{En} represents a VMD fit to early data below $Q^2 < 0.5$ (GeV/c)^2. It is in good agreement with the new higher Q^2 data.

Extensive studies of the model sensitivity of the extracted form factors were made. The sensitivity to three deuteron wave functions, Paris.[10] Bonn,[16] and Reid soft core,[17] was negligible. Results for three inelastic Fermi-smearing prescriptions[11] and two relativistic PWIA calculations[12,18] are summarized in Table II. The largest change occurs in G_{Mn} using the Gross relativistic model,[12] which gives increasingly smaller values as Q^2 increases. This is due primarily to changes in the magnitude, rather than the shape, of the modelled quasielastic peak.

Using the Keister relativistic model[18] results in smaller changes in G_{Mn}, and the trend with increasing Q^2 is opposite in sign to the Gross-Van Orden values. The form factors are less sensitive to the inelastic modelling, although the sensitivity increases with Q^2.

In conclusion, quasielastic e–d cross sections have been measured and Rosenbluth separations used to obtain R_L and R_T, at $Q^2 = 1.75$, 2.50, 3.25 and 4.00 (GeV/c)^2. Using a PWIA model, values for G_{En} and G_{Mn} have been extracted which greatly increase the Q^2 range of previous data with significantly smaller error bars. The results were found to be insensitive to three choices of the deuteron wave function. The modeling of the inelastic background has a small effect on the form factors, which increases with Q^2. Studies with two relativistic PWIA calculations indicate that G_{Mn} may be somewhat sensitive to relativistic corrections, especially at the highest Q^2. The effects of final state interactions and meson exchange currents may be important, and remain to be studied. The results for $G_{Mn}/\mu_n G_D$ are consistent with form factor scaling, and the results for G^2_{En}/G^2_D are consistent with zero. None of the theoretical models are in good agreement with the data for both form factors. It is possible that use of the new data to adjust free parameters may improve agreement for many of the models.

Table I. Results for $G_{Mn}/\mu_n G_D$ and G^2_{En}/G^2_D as a function of Q^2 in $(\mathrm{GeV/c})^2$. The first error is statistical only,and the second includes point-to-point and absolute systematic errors.

Q^2	$G_{Mn}/\mu_n G_D$	G^2_{En}/G^2_D
1.75	1.052 ±0.026 ±0.045	-0.008 ±0.074 ±0.117
2.50	1.014 ±0.017 ±0.041	-0.050 ±0.074 ±0.142
3.25	0.967 ±0.031 ±0.052	0.164 ±0.154 ±0.252
4.00	0.923 ±0.048 ±0.065	0.235 ±0.269 ±0.356

Table II. Results for $G_{Mn}/\mu_n G_D$ and G^2_{En}/G^2_D extracted with different models. Inel1, Inel2, and Inel3 indicate different inelastic Fermi-smearing models [11], with a non-relativistic quasielastic model. Keister [18] and Gross [12] indicate two relativistic quasielastic models, with inelastic model (Inel1). All calculations used the Paris wave function. Q^2 in units $(\mathrm{GeV/c})^2$.

Q^2	Inel1	Inel2	Inel3	Keister	Gross
		$G_{Mn}/\mu_n G_D$			
1.75	1.052	1.059	1.058	1.044	1.008
2.50	1.014	1.026	1.025	1.008	0.954
3.25	0.967	0.985	0.987	0.972	0.899
4.00	0.923	0.955	0.952	0.937	0.866
		G^2_{En}/G^2_D			
1.75	-0.008	0.002	0.022	-0.040	-0.010
2.50	-0.050	-0.015	-0.001	-0.082	-0.052
3.25	0.164	0.222	0.190	0.104	0.149
4.00	0.235	0.272	0.171	0.152	0.186

REFERENCES

a. Present address: California Institute of Technology, Pasadena, CA 91125.

b. Present address: Stanford Linear Accelerator Center, Stanford, CA 94309

c. Present address: George Washington University, Wash., D.C. 20052

d. Present address: Old Dominion University, Norfolk, VA 23529

1. G. Höhler *et al.*, Nucl. Phys. **B114**, 505 (1976). Fit 5.3.

2. G. P. Lepage and S. J. Brodsky, Phys. Rev. Lett. **43**, 545 (1979); **43**, 1625 (1979).

3. M. Gari and W. Krümpelmann, Z. Phys. **A322**, 689 (1985).

4. A. V. Radyushkin, Acta. Phys. Pol. **B15**, 403 (1984).

5. P. L. Chung and F. Coester, Phys. Rev. **D44**, 229 (1991). Model with $M_q = 0.24$.

6. S. Rock *et al.*, Phys. Rev. Lett. **49**, 1139 (1982).

7. W. Bartel *et al.*, Nucl. Phys. **B58**, 429 (1973).

8. P. E. Bosted *et al.*, Phys. Rev. Lett. **68**, 3841 (1992).

9. L. Durand III, Phys. Rev. Letters **6**, 631 (1961); I. McGee, Phys. Rev. **161**, 1640 (1967); **158**, 1500 (1967).

10. M. Lacombe *et al.*, Phys. Lett. **101B**, 139 (1981).

11. M. M. Sargsyan, L. L. Frankfurt, and M. I. Strikman, Z. Phys. **A335**, 431 (1990).

12. F. Gross and J. W. Van Orden, private communication.

13. R. G. Arnold *et al.*, Phys. Rev. Lett. **61**, 806 (1988).

14. A. S. Esaulov *et al.*, Yad. Fiz. **45**, 410 (1987).

15. S. Galster *et al.*, Nucl. Phys. **B32**, 221 (1971).

16. R. Machleidt *et al.*, Phys. Rep. **149**, 1 (1987).

17. R. Reid, Ann. Phys. **50**, 411 (1968).

18. B. D. Keister, private communication. See also Phys. Rev. **C37**, 1765 (1988).

ACKNOWLEDGEMENTS

We acknowledge the support of the SLAC management and staff, especially G. Davis, R. Eisele, C. Hudspeth, and J. Mark. We are grateful to F. Gross, B. D. Keister, M. Strikman, and J. W. Van Orden for providing numerical calculations and for valuable discussions.

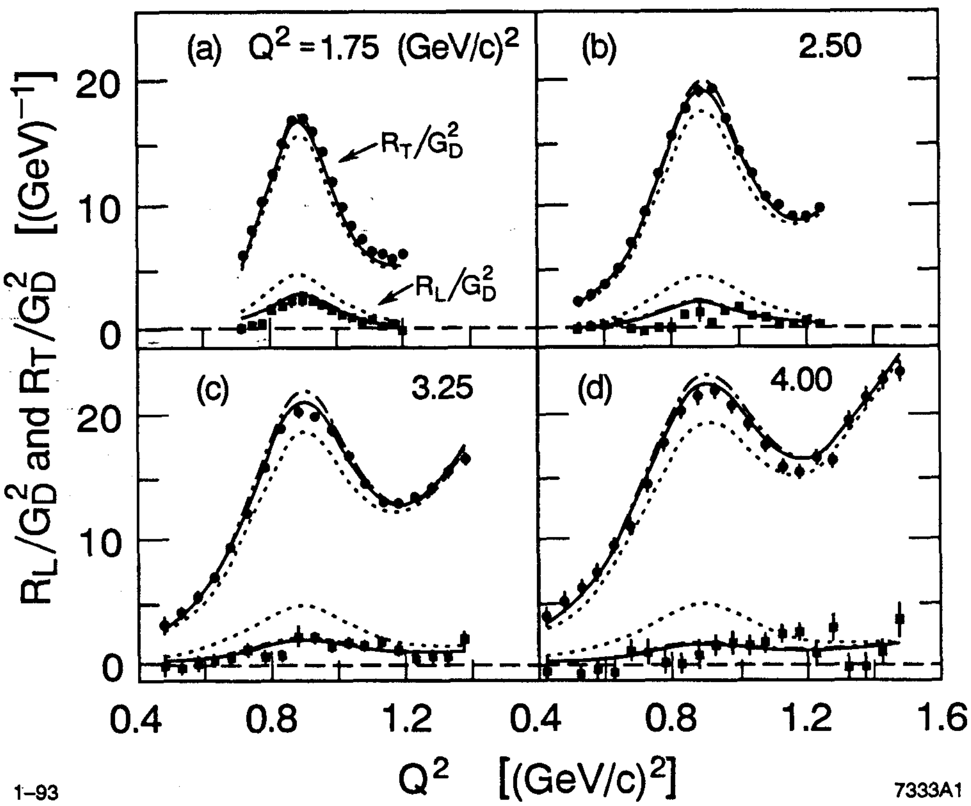

(a) $Q^2 = 1.75$ (GeV/c)^2
R_T/G_D^2
R_L/G_D^2
(b)
2.50
(c)
3.25
(d)
4.00
R_L/G_D^2 and R_T/G_D^2 [(GeV)$^{-1}$]
0
10
20
0.4
0.8
1.2
1.6
Q^2 [(GeV/c)^2]
1-93
7333A1

Fig. 1

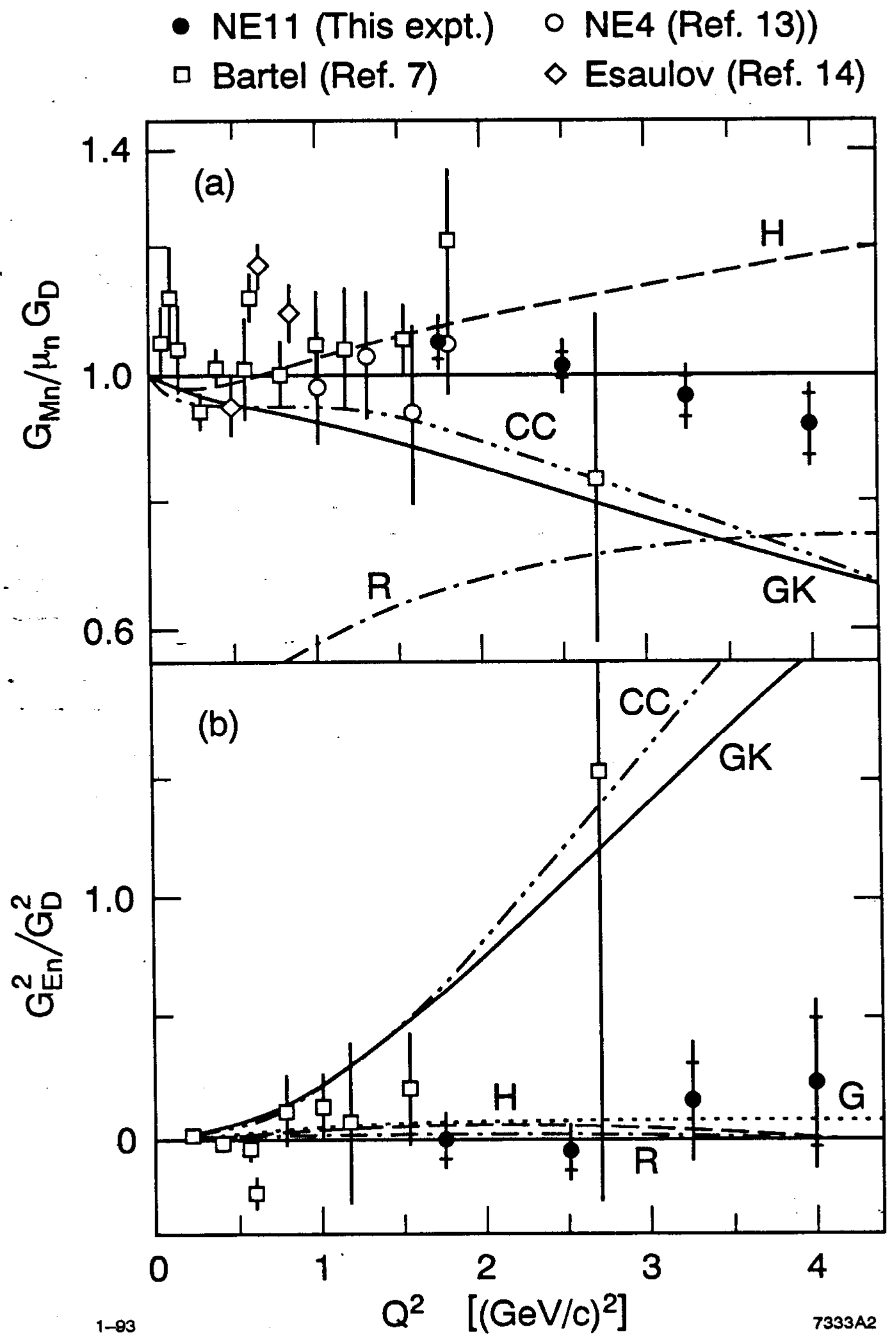

NE11 (This expt.)
NE4 (Ref. 13))
Bartel (Ref. 7)
Esaulov (Ref. 14)
(a)
(b)
H
CC
R
GK
G
1.4
1.0
0.6
0
1
2
3
4
$G_{Mn}/\mu_n G_D$
G_{En}^2/G_D^2
Q^2 [(GeV/c)^2]
1–93
7333A2

Fig. 2